integrity Research Journals

Global Journal of Earth and Environmental Science
Volume 5(4), pages 101-116, October 2020
Article Number: 016617043
ISSN: 2636-6002
https://doi.org/10.31248/GJEES2020.087
https://integrityresjournals.org/journal/GJEES

Full Length Research

Kinematic evolution of the Pan-African shear zones of South Maradi, southern Niger

Souley Baraou Idi[1]* and Moussa Konaté[2]

[1]Department of Geology, University of Agadez, Faculty of Sciences and Technology, P.O. Box 199, Agadez, Niger.
[2]Department of Geology, Abdou Moumouni University, P. O. Box 10662, Niamey, Niger.

*Corresponding author. Email: souleybaraou2@gmail.com

Received 13th October, 2020 ; Accepted 28th October, 2020

ABSTRACT: The Pan-African Province (PAP) of south Maradi (Niger) corresponds to the northeastern part of the Benin-Nigerian Shield, which is part of the Pan-African Mobile Belt, located to the East of the West African Craton. This study focuses on the microstructural study supported by geochronological data of the South Maradi Pan-African shear zones. The structural analysis of the Pan-African shear bands, combined with the previous radiometric data allowed to highlight a polyphase history of this northeastern part of the Benin-Nigerian Shield. Two major tectonic periods are highlighted: A ductile to brittle Pan-African deformation stage (D1) relayed by a brittle post-Pan-African deformation stage (D2). The first phase D1 consists of two episodes noted D1a and D1b: (1) the D1a episode was a ductile pan-African deformation stage with a strong coaxial component, which favoured the development of symmetric fabrics of foliation. The tectonic regime was characterized, first by a NW-SE (~N140°) trending pure-shear-dominated shortening episode, which prevailed between 617.9 ± 2.8 to 589 ± 1.9 Ma. Then during episode D1a, the shortening direction evolved gradually from NW-SE to ~E-W (N90°-N70°). This change of direction is due to the constraint coming from the Pan-African orogeny. The deformation had progressively a rotational component and this is how D1b episode began. This latter was characterized by a brittle-ductile deformation, associated with the formation of mylonitic gneiss and micaschist. So, the counter clockwise sinistral rotation of the shortening axis Z (from N140° to N90°- N70°) reveals a Pan-African continuum of deformation between D1a and D1b episode. (2). Subsequently, a stage of brittle deformation D2 affected all the previous structures. This D2 stage is marked by a continental-scale system of conjugated strike-slip faults, NE-SW and NW-SE trending. This investigation contribute to knowledge of Pan-African kinematic evolution of Benin-Nigerian Shield, particularly its northeastern part (South Maradi).

Keywords: Microstructural study, Pan-African province, Schist belt, Shear zone, South Maradi.

INTRODUCTION

This Pan-African Province of the South Maradi (Figure 1) was formed during the Pan-African orogeny (between 750 and 450 Ma, Ajibade and Wright, 1989), as the result of the convergence and the collision of the West African Craton (WAC), São Francisco Craton, Congo Craton and the Saharan Metacraton, in the context of West Gondwana amalgamation.

The present structural framework of the Southern Maradi Province (Figure 2) resulted from the Pan-African orogeny. It forms an alternatively juxtaposed domains of four NE-SW trending bands of schist belts with bands of banded granitic gneiss (with migmatite panels), associated with post-tectonic granitoid intrusions including pegmatites.

Previous works in the study area are limited respectively to the geological and airborne geophysical mapping of Mignon (1970) and PRDSM (2005). In addition, these two works have highlighted gold alluvium occurrences without any link with the basement deformations.

Unlike that of Benin-Nigerian Shield provinces, the tectonics of the PAP of the South Maradi, particularly the evolution of the major transcurrent shear zones structures have not been investigated and situated in their regional context.

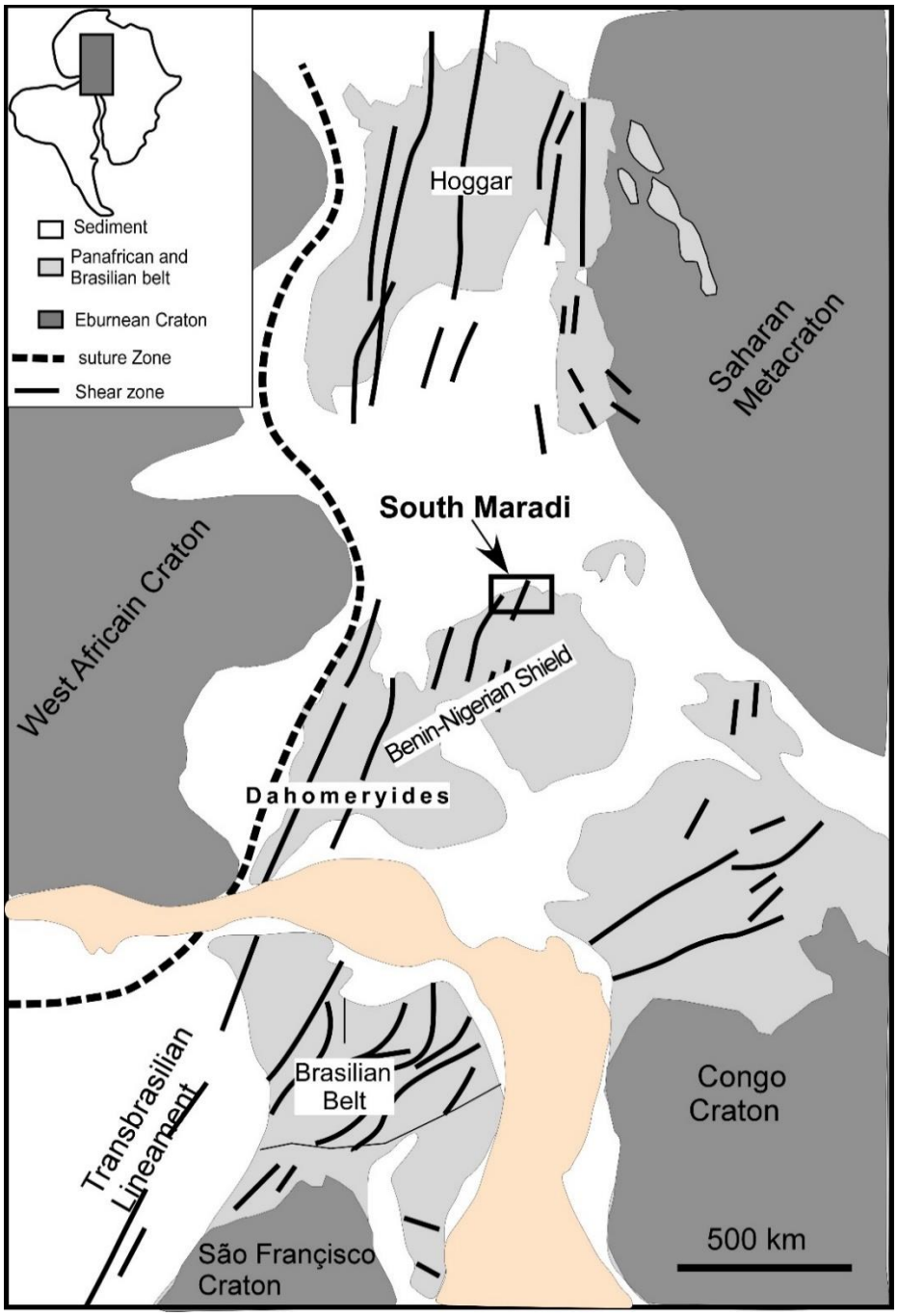

Figure 1. Geological reconstruction between Africa and Northeastern Brazil before the opening of the Atlantic Ocean (according to Caby et al., 1991).

This study is based on *in situ* microstructural analysis of South Maradi shear zones to determine the kinematic evolution of this region, hitherto less known at regional scale.

GEOLOGICAL SETTING

The outcropping rocks in the South Maradi consist mostly of schists, migmatitic gneiss, micashists, banded gneiss, granitic mylonitic gneiss, quartzites and post-tectonic granites including pegmatites dykes.

Four schist belts have been identified and named after the different localities where the outcrop is more important. From Southwest to Northeast: the Maraka (MSB), the Eastern Goumata (GSB), the Garin Liman (GLSB) and the Maidaparo (MpSB) schist belts are distinguished (Figure

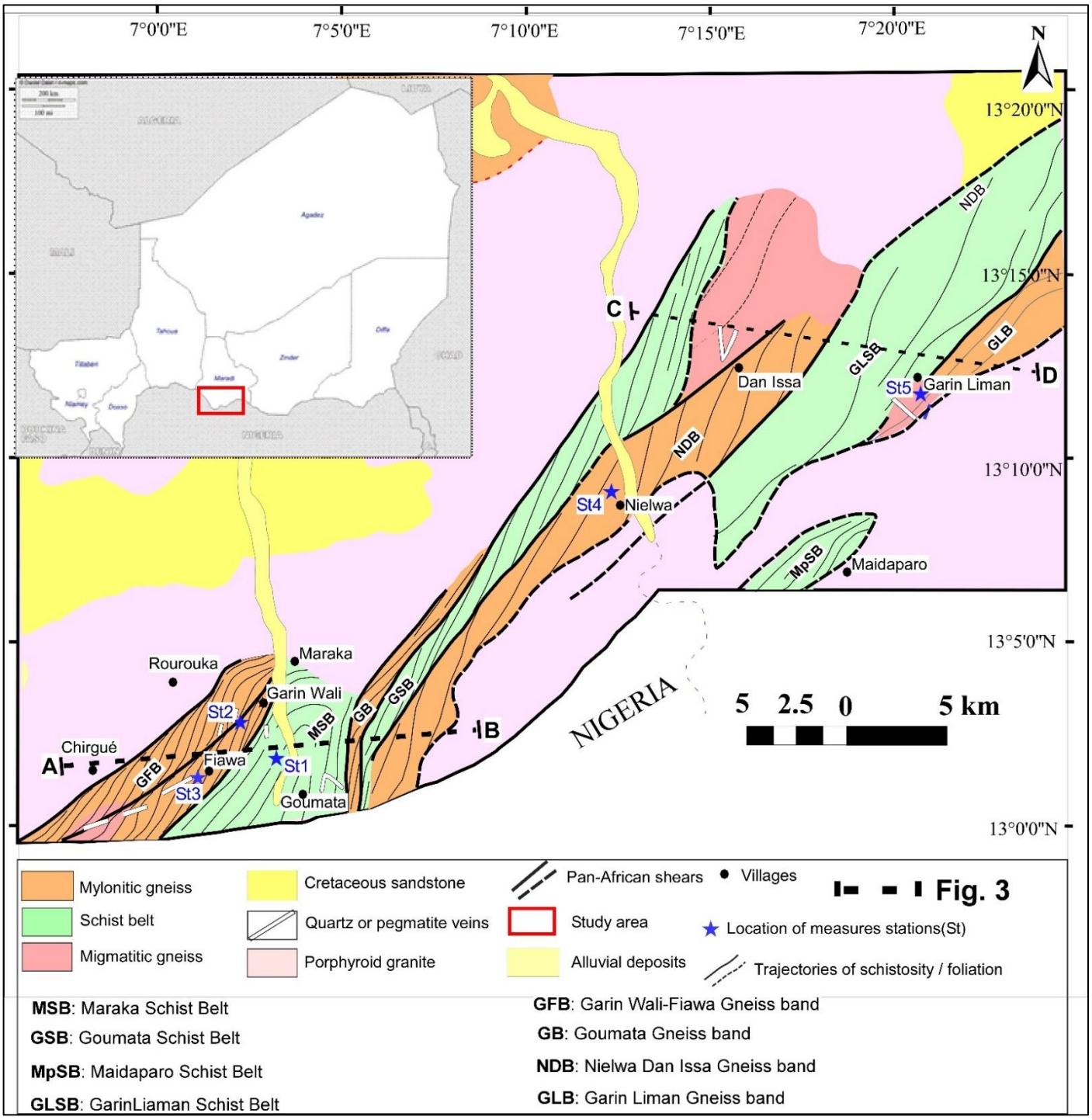

Figure 2. Geological map of the study area compiled from geophysical (PRDSM 2005) and cartographical data (Mignon, 1970), bore hole and field data (Baraou et al*.,* 2018), showing the location of dated samples by U-Pb method and K-Ar method and geological sections lines.

2). The schists are located mainly in the NE-SW trending belts with a metamorphic grade mostly within the green schist facies (Baraou et al., 2018). These schist formations were dated at 617.9 ± 2.8 Ma by using U-Pb zircon method and at 508 ± 10 Ma by using the K-Ar method on total rock (Table 1, Baraou and Konaté, 2020).

The schist belts are outcropping in the shape of alternating bands of about 1 to 5 km wide (Figure 2), and are bounded by mylonitic gneiss bands (Figure 2). Four bands of mylonitic gneiss were distinguished. These

Table 1. Recapitulative of available radiometric data in South Maradi (Baraou and Konaté, 2020).

Samples	Radiometric ages/method	Dated Material	Ages interpretation
Maraka schist	617.9 ± 2.8 (U-Pb)	Zircon	Age of the Pan-African ductile deformation (D1a), dominated by pure shearing
	505 ± 15 Ma (K-Ar)	Whole rock	Age of the Pan-African semi-ductile deformation (D1b), dominated by simple shearing
Dan Issa migmatite gneiss	589.6 ± 1.9 Ma (U-Pb)	Zircon	Age of Pan-African migmatization and mylonitization
Fiawa mylonitic gneiss	491 ± 10 Ma (K-Ar)	Feldspars	Age of the Latest Pan-African reactivation
Rourouka porphyric granite	508 ± 10 Ma (K-Ar)	Whole rock	Age of granitoid emplacement

include the Fiawa-Garin Wali (GFB), the Eastern Goumata (GB), the Nielwa-Dan Issa (NDB) and the Garin Liman (GLB) (Figure 2) (Baraou et al., 2018). Mylonitic gneiss occur in the NE-SW shear zones and extend into the neighboring Nigeria. The schist belts as well as the mylonitic gneiss are intruded by weakly deformed or undeformed granitoids (Mignon, 1970; PRDSM 2005; Baraou et al., 2018).

In the study area, the geological formations display a gradual transition from schist to gneiss and then to migmatite and granite (Figure 2). Three main lithostratigraphic units correlable with those of Northern Nigeria can be distinguished. They include:

(1) The migmatite-gneiss complex of Garin Wali and Garin Liman (PRDSM, 2005) corresponding to the "Migmatite-Gneiss Complex" of Northern Nigeria (Kennedy Grant, 1970, Oversby, 1975, Bruguier et al., 1994) (Figure 1). An age of 2700 Ma at 2000 Ma is attributed to the Northern Nigeria complex which corresponds to an older basement, representing blocks of Archean to Paleoproterozoic continental crust.
(2) The South Maradi Schists belts which have been dated at 617.9 ± 2.8 Ma by Baraou et al. (2018) using U-Pb zircon method and at 508 ± 10 Ma by the same author using the K-Ar method on total rock (Figure 1). The Maraka Schists belts for exemple represent the extension of the Wonaka Schist Belt of Northern Nigeria, for which an age of 496 ± 50 Ma (Rb-Sr method on total rock) was obtained by Ogezi (1977). According to Okonkwo and Ganev (2015), the Schist Belt formations would be old sediments infilling a pan-African basin, which would have undergone a metamorphism in the green schist facies.
(3) The Pan-African granitoids of Chirgué as well as the Nielwa-Dan Issa mylonitic gneiss (Figure 1) correspond to the "Older granites" of Nigeria (Mignon, 1970; PRDSM, 2005; Olusiji, 2013). The Dan Issa migmatite gneiss (South Maradi) gave a U-Pb age on recrystallized zircons of 589.6 ± 1.9 Ma which corresponds to the age of Pan-African ductile deformation (Baraou and Konaté, 2020). In the Jos Plateau of Nigeria. Ar-Ar age of 565 ± 5 Ma on Hornblende then and U-Pb age of 589 ± 11 Ma and 605 ± 10 Ma on zircon were attributed to this type of granitoids, respectively by Ferré et al. (2002), Dada and Respaut (1989) and Van Breemen et al. (1977).

Most of the geological formations and structures of Southern Maradi (Figure 2) are in continuity with those of northern Nigeria (Mignon, 1970, Ferré et al., 1996, 2002, PRDSM, 2005, Baraou et al., 2018). Geological works in the contiguous provinces of northern Nigeria explain the deformations in a context of polyphase tectonic event that affected the Benin-Nigerian Shield (Turner, 1983; Fitches et al*.,* 1985; Grant, 1970; Dada, 1998; Kröner et al*.,* 2001; Kennedy Grant, 1970; Oversby, 1975; Okonkwo and Ganev, 2015, Glodji, 2012). According to these previous authors, the polycyclic basement of Benin-Nigeria corresponds to an old reactivated crust including Archean (3571 ± 3 Ma to 2700 ± 200 Ma) and Paleoproterozoic panels (2330 ± 70 Ma) in Nigeria and (2091 ± 14 Ma) in Benin.

The Pan-African Orogeny (600 ± 150 Ma) is the latest reactivation that has affected the whole region (Turner, 1983; Fitches et al., 1985; Wright et al., 1985; Black, 1994). The latest Pan-African deformation event would be associated with the activation of pan-African shearing structures (ca. 505 ± 10 Ma K-Ar, in Southern Maradi, Baraou et al., 2018) and ca. 496 ± 50 Ma Rb-Sr in NW Nigeria, as suggested by Ogezi (1977). It played an important role in the circulation of mineralized fluids (Garba, 2002; Abubakar, 2012) and is marked by the formation of mylonites and cataclasites resulting from the shearing of rocks at different levels of the earth's crust. Kinematic markers show that dextral transcurrent displacement was important in the final amalgamation of different crustal blocks during the closing stages of the Pan-African Orogeny.

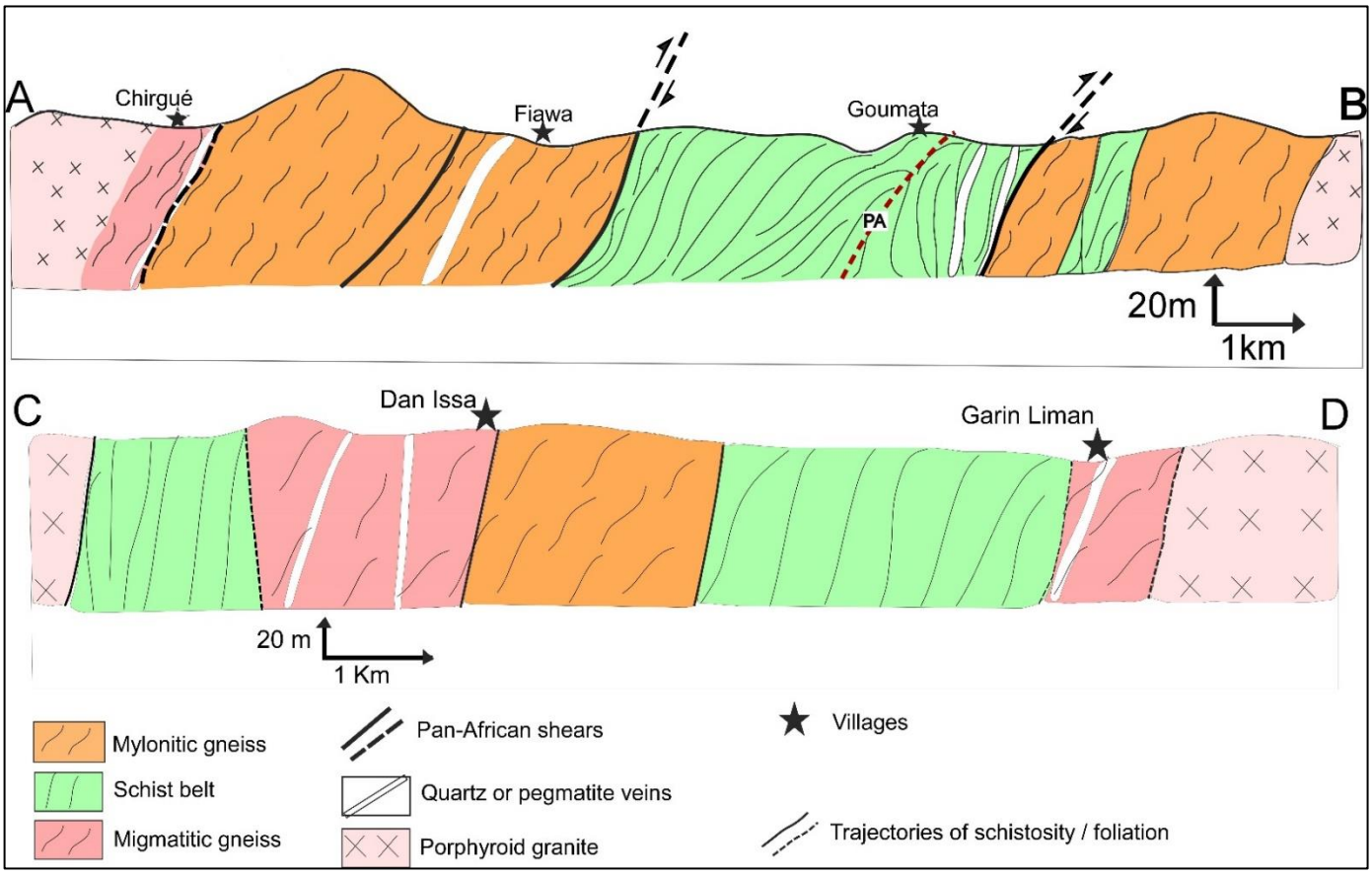

Figure 3. Geological sections (oriented E-W) showing the arrangement of South Maradi formations.

MATERIAL AND METHODS

The methodologic approach adapted involves *in-situ* observation, microtectonic analysis and studying of outcrops and their dispositions. The microtectonic data obtained are indictaed in the appendix part. The differents planes (schistosity, foliations, shear and fault plane planes) were analyzed by using Stereonet10 (Allmendinger et al., 2017). The interpretation of these structural data was based on the determination of shortening direction ($\sigma 1$) and its variation according to the analyzed petrofabric. The petrostructural data were combined with the previous radiometric data obtained by Baraou and Konaté (2020) in the same area to determine the chronology of different kinematic stages.

RESULTS

Structures of deformation

In the field, the most structure of deformation are described in the schist belts, mylonitic gneiss bands and migmatite gneiss. The Figure 3 shows the spatial arrangement of the studied formations.

Schist belts structures

In the schist belts, the deformation is marked by a symmetric and sub-vertical N30° to N50° trending S1 schistosity (Figure 4a-b, Appendix 1), in relation with a coaxial ductile deformation by pure flattening. The quasi-regularity of the S1 schistosity planes is associated with similar F1 folds whose subvertical axial planes (Figure 4c) have a N40° mean direction, which is parallel to the direction of the schistosity S1.

Banded and mylonitic gneiss

Banded gneiss are characterized by alternating quartzo-feldspathic and biotite beds defining a symmetrical N30° (Garin Wali, Figure 5a; Appendix, 2) to N50° trending foliation (Fiawa, Figure 5b; Appendix 3). This symmetrical foliation ("ϕ-type structure", Passchier and Trouw, 2005) was attributed to an episode of ductile coaxial deformation, by pure flattening, compatible with a N120° to N140° shortening direction.

In the mylonitic gneiss marked by N-S to N20° trending foliation, the ductile deformation has a rather non-coaxial component. The kinematic indicators include two kinds of structure:

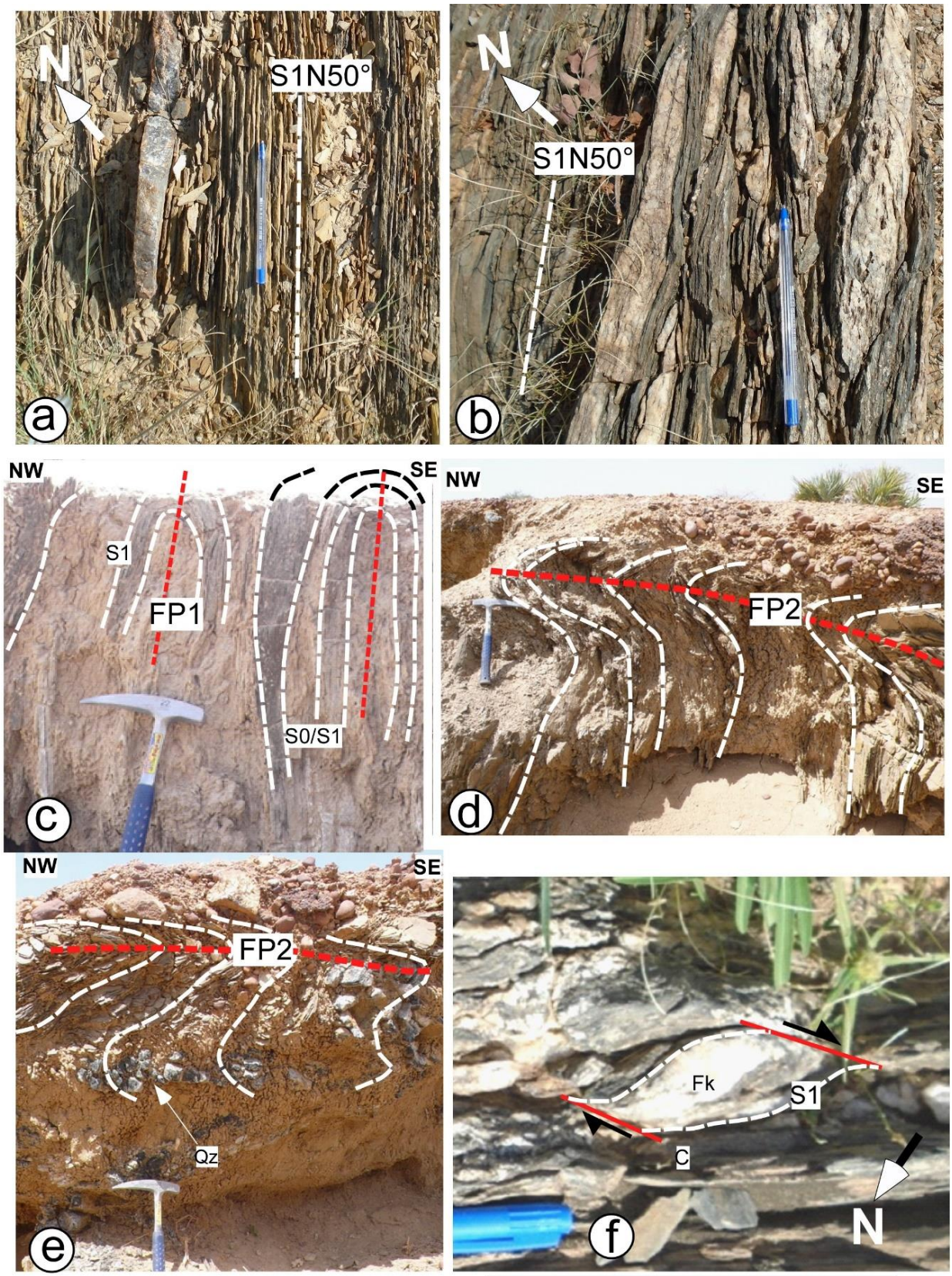

Figure 4. Detailed photographies of schist outcrops in the Maraka schist belt. In **a** and **b**: coaxial deformation by pure flattening, trajectory of S1 (schistosity / foliation). In **c**: FP1: subvertical to vertical axial plane. In **d** and **e**: FP2: subhorizontal axial plane of folded S1 schistosity. In **f**: A σ–type structure of a feldspar porphyroclast.

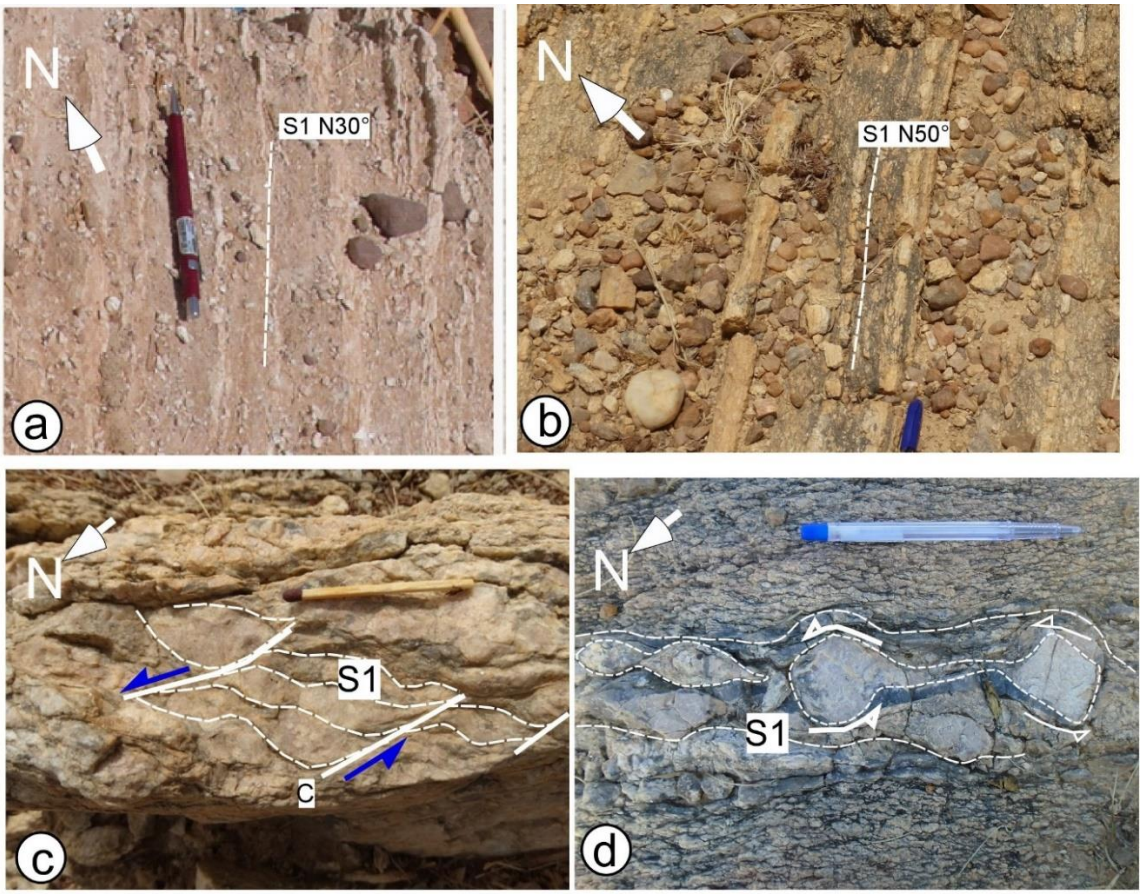

Figure 5. Detailed photographies of mylonitic gneiss of the Garin Wali and Fiawa areas showing a coaxial and non-coaxial deformation structures: (**a**) and (**b**) Symmetrical foliation boudinaged connected to a coaxial deformation by pure flattening. (**c**): sigmoid of feldspar porphyroclasts associated to a sinistral shearing sense. (**d**): Asymmetric foliation boudinage in amphibolite facies gneiss exhibiting a sinistral rotation of feldspar porphyroclast.

- On the one hand, the development of a S-C fabric ("σ-type structure", Passchier and Trouw 2005). The sigmoidal geometry of the porphyroclasts shows a sinistral rotational component, well pronounced in the pegmatitic gneiss (Figure 5c). This sigmoidal geometry is compatible with N-S to NE-SW compression.
- On the other hand, by asymmetric boudinage of potassium feldspars, associated with rotation features ("δ-type structure", Passchier and Trouw, 2005) (Figure 5d). The spiral shape of the rolling-up indicates a sinistral shear component, which is compatible with N-S to NE-SW compression axis.

In the Nielwa, Dan Issa and Goumata sectors, kinematic indicators in the mylonitic gneiss include sigma-type (σ-type) shape of pluricentimetric porphyroclasts, indicating a reactivation of S/C fabric in dextral sense (Figure 6; Appendix 4). The dextral sigmoidal geometry of some feldspar porphyroclasts marks as well as the transition from coaxial (Figure 4a-b) to non-coaxial deformation (Figure 5c-d and Figure 6).

Migmatic gneiss structures

In south Maradi, migmatites are characterized by a variety of petrographic facies (Figure 7) including porphyritic gneiss, leucosomes of aplitic granites and melanosomes of biotitite. In the migmatites of Garin Liman, the paleosomes are affected by anisopachous flow folds, with a strong dispersion of the fold axis (Figure 7a), showing a passage to anatexis granites (neosome). Chirgué migmatite gneiss (Figure 7b) consists of leucosomes of fine-grained gneiss and melanosomes represented by biotitite enclaves (Figure 7b). The microtectonic data of magmatic gneiss are indicated in Appendix 5.

Kinematic of the South Maradi shear zones

The geometric analysis of foliated and schistosed bands carried out in the case of this study, supported by previous radiometric data (Tabe 1) obtained by Baraou and Konaté (2020) allowed to highlight two major tectonic stages of kinematic evolution in South Maradi named D1 and D2.

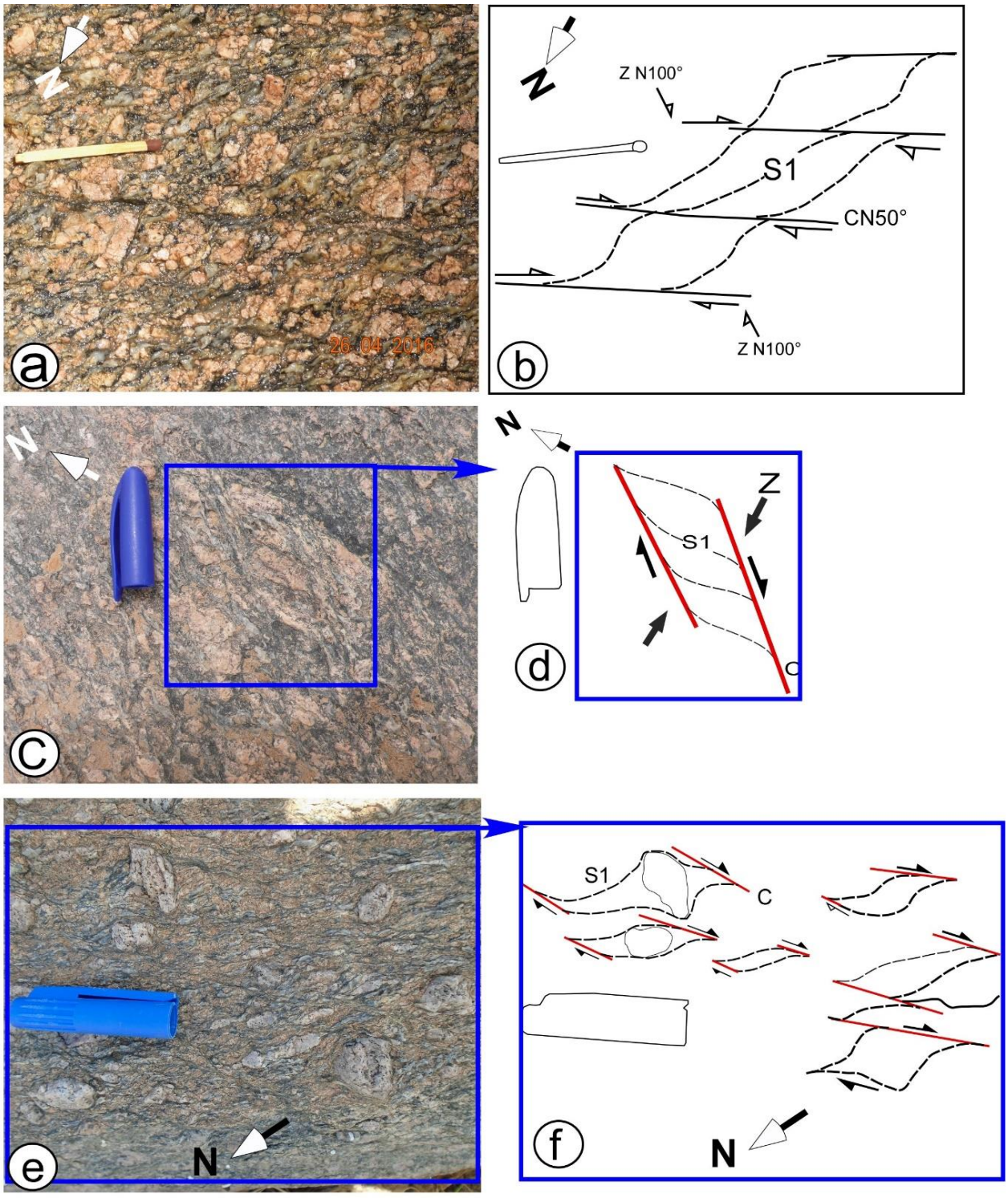

Figure 6. Detailed photographies of mylonitic orthogneiss of Dan Issa (**a**), Nielwa (**c**) and eastern Goumata areas (**e**) showing dextral shearing fabrics. **S1**: foliation trajectory. **C**: shear plane. **Z**: shortening direction.

The D1 Pan-African stage includes two episodes: D1a ductile and D1b semi-ductile. The D2 deformation stage, which was essentially brittle, assumed to be post-Pan-African.

First stage D1 (D1a and D1b)

Stage A: Between 617.9 ± 2.8 Ma and 589 ± 1.9 Ma (Baraou and Konaté, 2020), the southern Maradi NE-SW

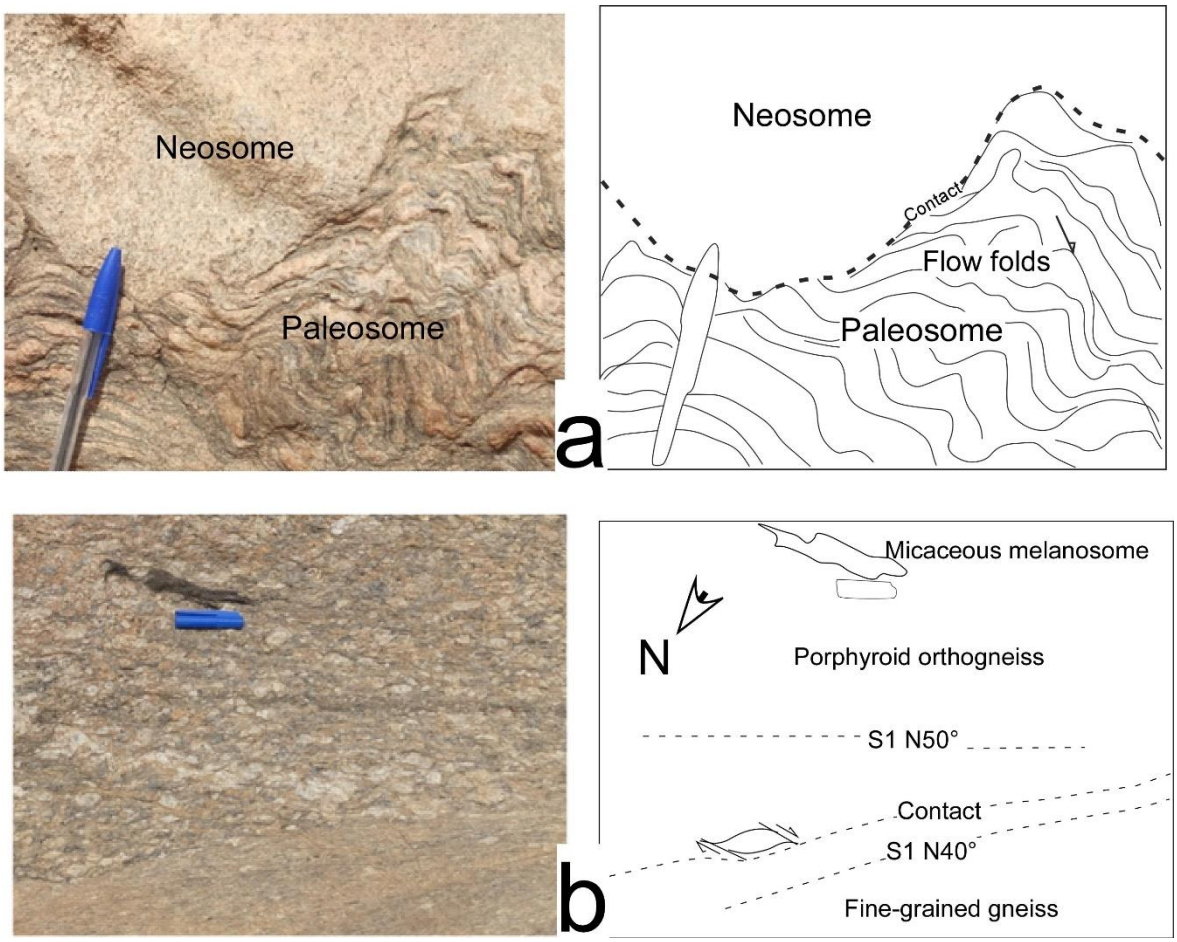

Figure 7. Photographies of migmatitite orthogneiss of Garin Liman (**a**) and migmatites of Chirgué (**b**). In (**a**): The paleosome is affected by asymmetric flow folds with strong dispersion of the fold axes, in close contact with an undeformed leucosome. In (**b**): A coarse-grained gneiss (paleosome) including rich micaceous melanosomes of biotite.

trending shear zones was affected by a ductile pure-shear-dominated deformation stage D1a, which had a coaxial component. As a result, the schistosity/foliation S1 ~ N50° striking was formed with some sub-isoclinal folds (Figure 8a,b,c). The shortening axis, deduced from the microtectonic analysis, was globally NW-SE (N140° to ~ N110°, Figure 8). This direction is nearby to N95° to N125° direction of the D1a episode obtained by Konaté (1996) in the northern Benin. The presence of these structures (schistosity/foliation S1, sub-isoclinal folds, asymmetric folds, sub-meridian shear) in South Maradi denotes a high tightening in a tangential tectonic context. In the South Maradi, this episode woud be associated to the emplacement of granitoid intrusions during the late pan-African events (Table 1).

It is important to note that during this D1a episode the sub-meridian structures was activated in sinistral (Figure 8f). The U-Pb dating on zircons of Maraka schist (Table 1) gave an age of 617.9 ± 2.8 Ma (Baraou and Konaté, 2020), corresponding to the first ductile deformation (D1a) that affected the the shear zones. This period of intense deformation (dated at 589 ± 1.9 Ma, U-Pb on zircons by Baraou and Konaté, 2020) is marked by migmatization, granitization and mylonitization (Figure 8e,f).

Stage B: The period between 505 ± 15 Ma and 491 ± 10 Ma (Baraou and Konaté, 2020) was characterized by a semi-ductile deformation dominated by simple shearing, named D1b. This second stage, inferred from the S-C structures of the shear zones, was related to a E-W to ENE-WSW compression direction (N90° to 0°). The deformation had a strong rotational component. The shear zones and the NE-SW to NNE-SSW trending strike-slip faults are dextrally reactivated (Figure 9a, b), developing locally a subhorizontal axial plane of S1 folded (Figure 9c). This second episode D1b is similar to the compression episode having the same direction N60° to N90°, highlighted in the basement of the Kandi Basin by Konaté (1996).The K-Ar age of 505 ± 15 Ma and 491 ± 10 Ma obtained respectively on schist and mylonitic gneiss were

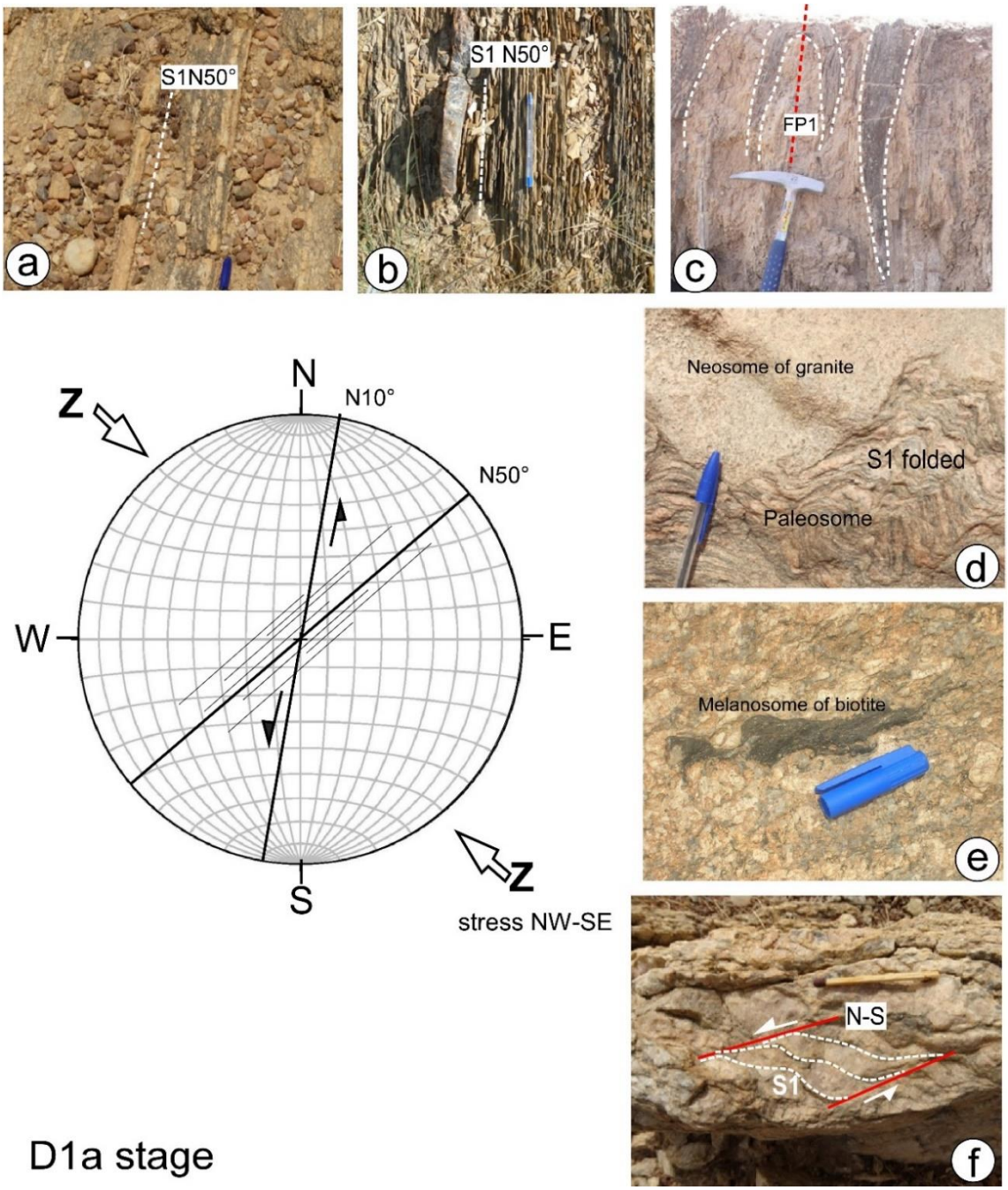

Figure 8. Structures of ductile deformation related to the D1a episode of shortening N140° trending.

attributed to this D1b episode. During the first deformation phase D1, the shortening axis had progressively a sinistral rotational movement and changed position from NW-SE (D1a stage) to W-E (D1b stage).

The rotation of compression axis explains the fact that at the regional scale the last stage of reactivation of the strike-slip faults and the ductile shear zones was associated with dextral mylonitization. This counter clockwise rotation of the direction of shortening reflects a continuum of deformation.

The observation of the mylonitic and schistosed zones in South Maradi shows that the nature of the reactivation of the shear zones, during the D1 compression phase, depends on their orientation with respect to the shortening axis Z (Figure 8). When it is oriented perpendicularly to the Z axis, it promotes the development of schistosity/foliation by pure shearing (Figure 8a,b,c). On the other hand, when it is oriented obliquely to the Z axis, it favors the development of S-C fabric with sinistral or dextral displacement.

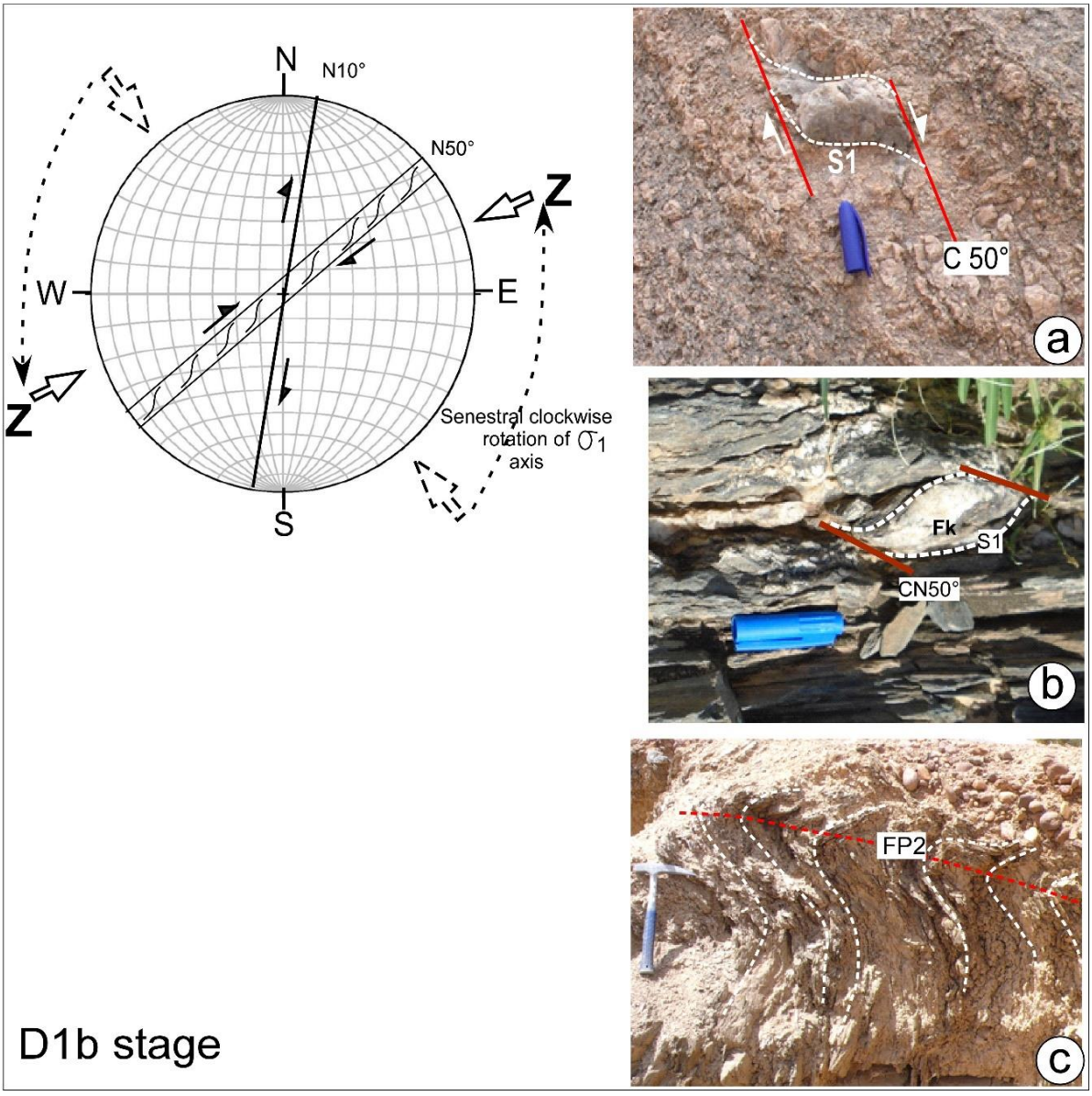

Figure 9. Ductile to semi-ductile deformation structures related to the D1b episode of shortening oriented N70° to N90°.

Second stage Brittle deformation D2

The second tectonic stage corresponds to a brittle deformation stage D2. It is considered by Ball (1980) as a late Pan-African fracture system. This deformation is associated, depending on the case, to many kinds of "strike-slip faults" or "fractures cleavage" S2 oriented N80° to N100° trend, displaced dextrally by S3 a "strain-slip" type schistosity, slightly dipping and oriented N40° (Figure 10). These later strike-slip faults with dextral displacement are conjugate with N110° to N140° sinistral trending faults (Figure 10). These sets of faults are similar to those described in the Tuareg shield. The dextral faults shows a NE-SW strike, and the sinistral faults a NW-SE strike (MC Curry, 1971; Ball 1980).

DISCUSSIONS

In the southern Maradi, the D1 Pan-African deformation phase includes two episodes : D1a and D1b. The first D1a stage is characterized by a coaxial deformation by pure shearing, along NE-SW trending shear zones, associated to the development of anisopachous folds. Analysis of the kinematic criteria along the sub-meridian transcurrent faults indicates a sinistral mylonitization. This NW-SE pure shear is comparable to the W-E compression direction obtained by Pires et al. (2016) in Brasília Fold Belt area and similar to the NW-SE tangential described by de Lira Santos et al. (2017) in the Borborema Province and nearly similar to the WNW-ESE to NW-SE direction obtained by Konaté (1996) in the Northern Benin. In addition, the D1a

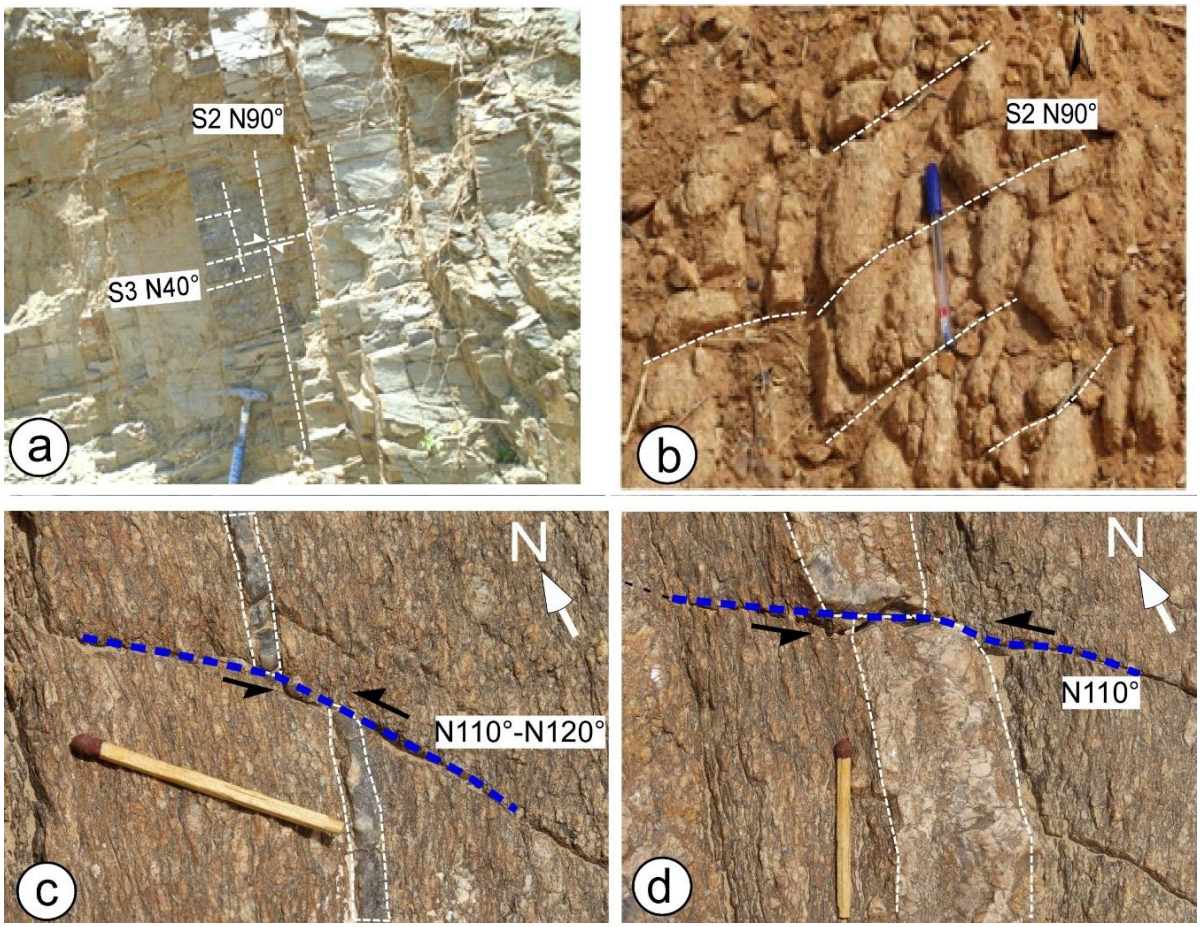

Figure 10. Detailed photographies showing brittle deformation structures affecting schists and gneiss. (a and b) fracture schistosity S2 of "cleavage fracture" type, subvertical, oriented N80° to N100°, displaced dextrally by the S3 "strain-slip" schistosity slightly dipping and striking N40°. (In c and d) sinistral strike-slip faults oriented N110° to N120°, (in e and f) N40° trending strike-slip faults.

deformation episode highlighted in South Maradi would have the same age (618 ± 10 Ma, Dada et al., 1993; and 640 ± 20 Ma, Ferré et al., 2002) obtained in PAP of Eastern Nigeria.

The second stage D1b, dated between 505 ± 15 Ma and 491 ± 10 Ma, is characterized by E-W to ENE-WSW compression which is similar to the NE-SW with dextral reactivation obtained by de Lira Santos et al. (2017) in the Borborema Province.

The sinistral rotation of the compression axis between D1a stage (NW-SE) and D1b stage (W-E) explains the fact that at the regional scale, the last phase of reactivation of the strike-slip faults and the shear zones is associated with dextral mylonitization (Figures 5 to 8). The change of direction from NW-SE to E-W observed in the studied area is due to the counter clockwise movement of the continental crustal blocks (West African Craton, Congo Craton and São Francisco Craton).

This counterclockwise rotation of the compression axis resulted from the Pan-African deformation as suggested by Ferré et al. (2002) in Nigeria, Konaté (1996) in North Benin and Blanquat and Tikoff (1997) and Liégeois et al. (1994) in Aïr-Hoggar. The deformation phases D1 and D2 are generally recognized by most of the authors (Dumont et al., 1985; Caby and Boessé, 2001; Mvondo et al., 2003; Nzenti et al., 2006; Tairou et al., 2007; Chala et al., 2015). For these authors, the D1 deformation phase is associated with tangential tectonics whereas the deformation phases D2, D3, D4 and D5 (Dn + 4) are associated with transcurrent tectonics, related to the activation of continental-scale shear zones and faults. The D1b episode of mylonitization is related to the reactivation of large shear zones oriented N50°, which would be associated with the emplacement of granitoids around 508 Ma, the K-Ar age. This is well recorded by the porphyroid granite of Rourouka.

The polyphased characters between Pan-African/ Brasiliano Province (PABP) and WAC could be explained as the result of the convergence and the collision of the West African Craton (WAC), São Francisco Craton, Congo Craton and the Saharan Metacraton, in the context of West Gondwana amalgamation (Ajibade and Wright, 1989).

Conclusion

Structural data analysis supported by radiometric data provided insight into the geodynamic evolution of the South Maradi PAP. Indeed, the structural evolution of this province is marked by a polyphase tectonic including two main phases of deformation D1 and D2.

The D1 phase is a continuum of deformation including two stages that started by a coaxial to non-coaxial deformation D1a, relayed by D1b non-coaxial deformation. The first D1a stage, dated between 638 and 589 ± 1.9 Ma (age U-Pb from zircon), is marked by a tangential to oblique tectonic. It corresponds to a ductile deformation episode related to a NW-SE (140°) compression axis.

During the second stage D1b, corresponding to the late pan-African oblique tectonic, dated between 505 Ma and 491 Ma, the mean stress axis of compression which was ~ N140°, deviates progressively according to sinistral rotation towards the azimuth N70°-N90°. This D1b episode was characterized by a significant mylonitization, the N-S and NE-SW trending continental-scale shear zones and faults display a dextral sense. The change in the direction of deformation is due to the counter clockwise movement of the continental crustal blocks (West African Craton, Congo Craton and Sao Francisco Craton) during the Pan-African orogeny.

The last phase D2 of the structural evolution is marked by a conjugated system of fractures affecting all previous pan-African structures. This second phase D2 is interpreted as a late to Post pan-African period of brittle tectonics, associated to a compression globally E-W trend.

This study constitute a modest contribution to the knowledge of Pan-African kinematic evolution in Benin-Nigerian Shield, particularly in its northeastern part (South Maradi). In prospect, investigations will be continued in the same area for further details.

CONFLICT OF INTEREST

The authors declare that they have no conflict of interest.

REFERENCES

Abubakar. Y. I., (2012). An integrated technique in delineating structures: A Case study of the Kushaka Schist Belt Northwestern Nigeria. *International Journal of Applied Science and Technology*, 2(5), 164-173.

Ajibade, A. C., & Wright, J. B. (1989). The Togo-Benin-Nigeria Shield: evidence of crustal aggregation in the Pan-African belt. *Tectonophysics*, 165(1-4), 125-129.

Allmendinger, R. W., Cardozo, N., & Fisher, D. (2017), Structural geology algorithms: Vectors and tensors in structural geology: Cambridge University Press.

Ball, E. (1980). An example of very consistent brittle deformation over a wide intracontinental area: the late Pan-African fracture system of the Tuareg and Nigerian shield. Tectonophysics, 61(4), 363-379.

Baraou, I. S., & Konaté, M. (2020). New radiometric data from the South Maradi Pan-African formations, southern Niger. *Geological Society, London, Special Publications*, 502.

Baraou, I. S., Konaté, M., Ahmed, Y., & Abdoul. W. D. (2018). Caractérisation de la déformation du socle de la zone mobile panafricaine du Sud Maradi, Sud Niger. *Afrique Science,* 14(1), 156-170.

Black, R., Latouche, L., Liégeois, J. P., Caby, R., & Bertrand, J. M. (1994). Pan-African displaced terranes in the Tuareg shield (central Sahara). *Geology*, 22(7), 641-644.

Blanquat, S, M., & Tikoff, B. (1997). Development of magmatic to solid-state fabrics during syntectonic emplacement of the Mono Creek granite, Sierra Nevada Batholith. In: Bouchez, J. L., Hutton, D. H. W., & Stephens, W.E. (eds.), *Granite from Segregation of Melt to Emplacement Fabrics. Petrology and Structural Geology*. Kluwer Publishing Co, Dordrecht. Pp. 231-252.

Caby, R., & Boessé J. M. (2001). Pan-African nappe system in southwest Nigeria: the Ife-llesha schist belt. *Journal of African Earth Sciences*, 33(2), 211-225.

Caby, R., Sial, A.N., Arthaud, M.H., & Vauchez, A. (1991). Crustal evolution and the Brasiliano Orogeny in Nort-east Brazil. In: Dallmeyer, R. D. & Lécorché, J. P. (eds). *The West African Orogens and Circum-Atlantic Correlatives*. Springer, Berlin. Pp. 373-397.

Chala, D., Tairou, M. S., Wenmenga, U., Kwekam, M., Affaton, P., Kalsbeek, F., Tossa, C., & Houéto, A. (2015). Pan-African deformation markers in the migmatitic complexes of Parakou–Nikki (Northeast Benin). *Journal of African Earth Sciences*, 111, 387-398.

Dada, S. S. (1998). Crust-forming ages and proterozoic crustal evolution in Nigeria: a reappraisal of current interpretations. *Precambrian Research*, 87, 65-74.

Dada, S. S., Tubosun, I. A., Lancelot, J. R., & Lar, A. U. (1993). Late Archaean U□ Pb age for the reactivated basement of Northeastern Nigeria. *Journal of African Earth Sciences (and the Middle East)*, 16(4), 405-412.

Dada, S., & Respaut, J. P. (1989). La monzonite à fayalite de Bauchi Bauchite, nouveau témoin d'un magmatisme suntectonique pan-africain au nord du Nigeria. *Comptes rendus de l'Académie des sciences. Série 2, Mécanique, Physique, Chimie, Sciences de l'univers, Sciences de la Terre*, 309(9), 887-892.

de Lira Santos, L. C. M., Dantas, E. L., Vidotti, R. M., Cawood, P. A., dos Santos, E. J., Fuck, R. A., & Lima, H. M. (2017). Two-stage terrane assembly in Western Gondwana: Insights from structural geology and geophysical data of central Borborema Province, NE Brazil. *Journal of Structural Geology*, 103, 167-184.

Dumont, J. F., Toteu, S. F., & Penaye, J. (1985). Ensembles structuraux et principales phases de déformations panafricaines dans la zone mobile du Nord Cameroun, région de Poli. *Revue Science et Technique. Série Sciences de la Terre*, 1(1/2), 9-23.

Ferré, E., Déléris, J., Bouchez, J. L., Lar, A. U., & Peucat, J. J. (1996). The Pan-African reactivation of Eburnean and Archaean provinces in Nigeria: structural and isotopic data. *Journal of the Geological Society*, 153(5), 719-728.

Ferré, E., Gleizes, G., & Caby, R. (2002). Obliquely convergent tectonics and granite emplacement in the Trans-Saharan belt of Eastern Nigeria: a synthesis. *Precambrian Research*, 114(3-4), 199-219.

Fitches, W. R., Ajibade, A. C., Egbuniwe, I. G., Holt, R. W., & Wright, J. B. (1985). Late Proterozoic schist belts and

plutonism in NW Nigeria. *Journal of the Geological Society, London*, 142(2), 319-337.
Garba, I. (2002). Geochemical characteristics of the gold mineralization near Tsohon Birnin Gwari, northwestern Nigeria. *Chemie der Erde*, 62(2), 160-170.
Glodji, L. A. (2012*). La zone de cisaillement de Kandi et le magmatisme associé dans la région de Savalou-Dassa (Bénin): étude structurale, pétrologique et géochronologique*. Thèse de Doctorat, Université de Lyon, 224 pages.
Kennedy Grant, N. (1970). Geochronology of precambrian basement rocks from Ibadan, southwestern Nigeria. *Earth and Planetary Science Letters*, 10(1), 29-38.
Konaté, M. (1996). Evolution Tectono-sédimentaire du Bassin Paléozoïque de Kandi (Nord Bénin, Sud Niger): Un témoin de l'extension post-orogénique de la chaîne panafricaine. Thèse de Doctorat de l'Universités de Bourgogne, Lyon I, Aix-Marseille I, Toulouse III. Premier Volume, 312p.
Kröner, A., Ekwueme, B. N., & Pidgeon, R. T. (2001). The oldest rocks in West Africa: SHRIMP zircon age for early Archean migmatitic orthogneiss at Kaduna, northern Nigeria. *The Journal of Geology*, 109(3), 399-406.
Liégeois, J. P., Black, R., Navez, J., & Latouche, L. (1994). Early and late Pan-African orogenies in the Air assembly of terranes (Tuareg Shield, Niger). *Precambrian research*, 67(1-2), 59-88.
Mc Curry, P. (1971). Pan-African orogeny in northern Nigeria. *Geological Society of America Bulletin*, 82(11), 3251-3262.
Mignon, R. (1970). Etude géologique et prospection du Damagaram Mounio et du Sud Maradi. *Rapp. Bur. Rech. géol. Minière, Dir. Mines Géol., Niamey*. Pp. 46-54.
Mvondo, H., Den Brok, S. W. J., & Ondoa, J. M. (2003). Evidence for symmetric extension and exhumation of the Yaounde nappe (Pan-African fold belt, Cameroon). *Journal of African Earth Sciences*, 36(3), 215-231.
Nzenti, J. P., Kapajika, B., Wörner, G., & Lubala, T. R. (2006). Synkinematic emplacement of granitoids in a Pan-African shear zone in Central Cameroon. *Journal of African Earth Sciences*, 45(1), 74-86.
Ogezi, A. E. O. (1977). Geochemistry and geochronology of basement rocks from north western Nigeria. Ph.D. Thesis, Leeds University.
Okonkwo, C. T., & Ganev, V. Y. (2015). Geochemistry and geochronology of orthogneisses in Bode Saadu area, southwestern Nigeria and their implications for the Palaeoproterozoic evolution of the area. *Journal of African Earth Science*, 109, 131-142.
Olusiji, S. A. (2013). Geology and structure of the Precambrian rocks in Iworoko, Are, and Afao Area, Southwestern, Nigeria. *International Research Journal of Natural Sciences*, 1(1), 14-29.
Oversby, V. M. (1975). Lead isotope studies of aplites from the Precambrian basement rocks near Ibadan, S. W. Nigeria. *Earth Planetary Science Letters*, 27, 177-180.
Passchier, C. W., & Trouw R. A. J. (2005). *Microtectonics* (Second edition), Springer-Verlag, Berlin.
Pires, G. L. C., Everton, M. B., Christophe, R., Débora, B. N., & Maurício, P. (2016). Structural and lithological controls of goldebearing veins associated with the Brasiliano-Pan African Orogeny: An example from the Buracão Area, Araí Group (Brasília Fold Belt, Brazil). *Journal of South American Earth Sciences*, 66, 180-195.
PRDSM (2005). Projet de géophysique aéroportée dans le secteur Sud Maradi. Ministère des Mines et de développement Industriel. 55p.
Tairou, M. S., Affaton, P., Gélard, J. P., Aïté, R., & Sabi, B. E. (2007). Panafrican brittle deformation and palaeostress superposition in northern Togo (West Africa). *Comptes Rendus Geoscience*, 339(13), 849-857.
Turner, D. C. (1983). Upper Proterozoic Schist Belts in the Nigerian Sector of the Pan-African Province of West-Africa. *Precambrian Research*, 21(1-2), 55-79.
Van Breemen, O., Pidgeon, R. T., & Bowden, P. (1977). Age and isotopic studies of some Pan-African granites from North-central Nigeria. *Precambrian Research*, 4(4), 307-319.
Wright, J. B., Hastings, D. A., Jones, W. B., & Williams, H. R. (1985). *Geology and mineral resources of West Africa*. Allen and Urwin, London, 187p.

APPENDIX LIST

Appendix 1. Microtectonic data of Maraka schists belt.

St1	N13°59'41.2''	E7°2'43.5''	Maraka
N0	Direction	Dip	Dip sector
1	45°	80	SE
2	50°	85	SE
3	40°	60	SE
4	50°	55	NW
5	45°	70	NW
6	40°	90	E
7	50°	55	NW
8	40°	50	NW
9	45°	60	SE
10	40°	90	E
11	50°	90	W
12	50°	80	SE
13	45°	85	SE
14	40°	70	SE
15	45°	80	SE
16	30°	90	E
17	40°	65	SE
18	55°	80	SE

Appendix 2. Microtectonic data of Garin Wali mylonitic gneiss.

St2	N13°3'11.9''	E7°2'36.2''	Garin Wali
N0	Direction	Dip	Dip sector
1	25°	85	NE
2	15°	90	E
3	20°	80	NE
4	10°	70	E
5	20°	60	W
6	0°	45	E
7	10°	45	E
8	15°	50	E
9	0°	75	E
10	0°	70	E
11	10°	80	E
12	15°	60	W
13	20°	70	W
14	15°	90	E
15	20°	90	E
16	30°	80	W
17	10°	90	E
18	25°	80	E
19	25°	90	E
20	20°	85	E
21	10°	90	E
22	15°	75	NW

Appendix 3. Microtectonic data of Fiawa mylonitic gneiss.

St3	N13°1’24.2"	E7°1’42.3’’	Fiawa
N0	Direction	Dip	Dip sector
1	45°	40	E
2	30°	40	SE
3	20°	30	E
4	50°	50	SE
5	45°	50	E
6	45°	90	E
7	55°	90	E
8	45°	70	SE
9	50°	90	E
10	55°	80	NE
11	50°	90	E
12	45°	80	W
13	55°	90	W

Appendix 4. Microtectonic data of Nielwa-Dan Issa mylonitic gneiss.

St4	N13°8’24,6’’	E7°12’27,6’’	Nielwa
N0	**Direction**	**Dip**	**Dip sector**
1	55°	75	SW
2	45°	80	SE
3	60°	70	SW
4	55°	85	NE
5	50°	70	N
6	50°	70	NE
7	45°	80	SW
8	50°	70	SW

Appendix 5. Microtectonic data of Garin Liman migmatite gneiss.

St5	N13°11’23,4’’	E7°20’23,7’’	Garin Liman
N0	Direction	Dip	Dip sector
1	170°	30	W
2	140°	15	SW
3	130°	35	W
4	135°	20	SW
5	130°	60	SW
6	120°	40	SW
7	120°	55	SW
8	75°	50	SW
9	90°	60	S

Appendix 6. Brittle deformation planes.

N0	Direction	Dip	Dip sector
1	N60°	70	N
2	100°	70	N
3	90°	80	N
4	120°	90	E
5	110°	90	N
6	80°	85	S